

Copy 237  
RM L53G13a

Copy 237

RM L53G13a

NACA RM L53G13a

7448

## THEATRE



88 EHTON

卷之三

TECH LIBRARY KAFB-NM

# RESEARCH MEMORANDUM

# NOTES ON DAMPING IN ROLL AND LOAD DISTRIBUTIONS IN ROLL AT HIGH ANGLES OF ATTACK AND HIGH SUBSONIC SPEED

By Richard E. Kuhn

Langley Aeronautical Laboratory  
Classification cancel Langley Field, Va. *UNCLASSIFIED*  
By Authority of *Mr. T. H. P. B. Amendment to*  
(OFFICER AUTHORIZED TO CHANGE)

By ..... NAME AND ..... *John May 57*

1000 Pcs

.....  
**GRADE OF OFFICER MAKING CHANGES**

31 MAR 61 [REDACTED]

11. *W. C. W. (W. C. Williams)* (1870-1943) was a poet, novelist, and short story writer.

## ATIONAL ADVISORY COMMIT

# NATIONAL ADVISORY COMMITTEE FOR AERONAUTICS

## WASHINGTON

August 27, 1953

**RECEIPT SIGNATURE  
REQUIRED**



0144388

## NATIONAL ADVISORY COMMITTEE FOR AERONAUTICS

## RESEARCH MEMORANDUM

## NOTES ON DAMPING IN ROLL AND LOAD DISTRIBUTIONS IN ROLL

## AT HIGH ANGLES OF ATTACK AND HIGH SUBSONIC SPEED

By Richard E. Kuhn

## SUMMARY

Results are presented of an experimental investigation conducted in the Langley high-speed 7- by 10-foot tunnel of the damping-in-roll characteristics of a series of wing plan forms at angles of attack up to  $13^{\circ}$  and Mach numbers to 0.91. Included also is the spanwise load distribution obtained on one of these wings while rolling.

The results indicate that a large loss in damping occurs at successively lower angles of attack as the Mach number is increased. For swept wings which are subject to pitch-up tendencies, loss of damping occurs at about the angle of attack for pitch-up and those devices which alleviate pitch-up are similarly effective in improving the damping. A procedure is given whereby a satisfactory estimate of the spanwise load distribution can be made if the measured pressure-distribution data in pitch are available.

## INTRODUCTION

A considerable amount of effort has been expended in the past on experimental investigations of the damping-in-roll characteristics of various wing plan forms. These investigations have been largely confined to the variation with angle of attack at low Mach numbers (for example, refs. 1 to 7) or the variation with Mach number at low angles of attack (refs. 8 to 20). An indication of the range of these data is presented in figure 1.

Recently an investigation has been conducted in the Langley high-speed 7- by 10-foot tunnel of the characteristics in roll of several wings. Results for an angle-of-attack range from  $0^{\circ}$  to  $13^{\circ}$  were obtained at Mach numbers up to 0.91. For one of the wings, pressure distributions were measured during roll. Since some of the results obtained in the investigation are regarded as being very significant, the present paper was prepared in order to summarize some of the more important findings.

## COEFFICIENTS AND SYMBOLS

The coefficients and symbols used are defined as follows.

$C_L$	lift coefficient, perpendicular to relative wind, Lift/qS
$C_m$	pitching-moment coefficient, Pitching moment/qS $\bar{c}$
$C_l$	rolling-moment coefficient, about an axis parallel to the relative wind, Rolling moment/qS $b$
A	aspect ratio
S	wing area, sq ft (2.25 sq ft for all models)
b	wing span, ft
c	local wing chord, ft
$\bar{c}$	wing mean aerodynamic chord, ft.
$c_{av}$	wing average chord, ft
q	dynamic pressure, $\frac{1}{2}\rho V^2$ , lb/sq ft
V	free-stream velocity, ft/sec
$\rho$	air density, slug/cu ft
M	Mach number
$\alpha$	angle of attack, deg
$\Lambda$	sweep angle, deg
$\frac{pb}{2V}$	wing-tip helix angle, radians
p	rolling velocity, radians/sec
$c_n$	local section normal-force coefficient
y	spanwise distance from plane of symmetry, ft

$$C_{l_p} = \frac{\partial C_l}{\partial \frac{pb}{2V}}$$

## MODELS AND TESTS

The models tested included an unswept wing, two swept wings, and one triangular wing each in combination with a common fuselage. The principal geometric characteristics of the wings are given in table I. Ordinates of the fuselage are presented in reference 21. The models were tested on the Langley high-speed 7- by 10-foot tunnel forced-rotation apparatus (ref. 22). The Reynolds number range covered for each of the wings is presented in table I.

A pressure-switch assembly and eight electrical pressure gages were installed in the fuselage to transmit the pressure-distribution data from the rolling wing. The electrical signals from the pressure gages were taken through the slip rings and brushes of the forced-roll apparatus. Because of the limited number of slip rings, it was necessary to use a gang of special pressure switches geared together to connect the pressure orifices in the wing to the electrical gages in successive groups. The pressure data were recorded on a multiple-channel recording galvanometer.

## CORRECTIONS

The angle of attack of the model has been corrected for the deflection of the support system under load and for the effects of boundary-induced upwash by the method of reference 23. The blocking corrections which were applied to the dynamic pressure and Mach number were determined by the method of reference 24.

## DISCUSSION

## Measured Damping Characteristics

The damping-in-roll characteristics of the  $45^{\circ}$  swept wing (fig. 2) indicate that a serious loss of damping occurs at successively lower angles of attack as the Mach number is increased. At the lower Mach numbers (the data for  $M = 0.2$  were obtained from ref. 25), the loss in damping does not occur until after the angle of attack for maximum lift has been considerably exceeded. At the higher Mach numbers the loss in damping occurs at angles of attack below the maximum lift.

Figure 3 shows results for several wings of various plan forms at a Mach number of 0.85. As can be seen, the results indicate poor damping for all the wings in about the same angle-of-attack range. Note also that for the swept plan forms maximum lift has not been reached when this

loss in damping occurs. As would be expected, however, the loss in damping for the unswept wing occurs at an angle of attack slightly above that for the peak in the lift curve.

In the region of instability or very low damping, the variation of rolling moment with rolling velocity was found to be rather erratic, and it is difficult to determine what the effective value of the damping coefficient should be under such conditions. Some typical variations of rolling-moment coefficient  $C_l$  with wing-tip helix angle  $pb/2V$  are shown in figure 4. At zero angle of attack the variation is quite linear and a stable slope is shown for all wings. These favorable characteristics, however, are maintained only up to an angle of attack of  $6^\circ$  or  $8^\circ$ .

At an angle of attack of  $11^\circ$  the unswept-wing data exhibit a pronounced hysteresis. The data points for the curve were taken in the direction shown by the arrows. It should be remembered, of course, that the angle of attack of  $11^\circ$  for this wing is above the stall at the Mach number selected. For the other wings however maximum lift is obtained at an angle of attack considerably above  $11^\circ$ .

The  $32.6^\circ$  swept wing shows a definite instability over a wide range of rolling velocities. Of the wings tested, this plan form showed the most instability and the instability covered the largest ranges of Mach number and angle of attack.

The  $45^\circ$  swept wing shows a very large reduction in damping, but no hysteresis, at an angle of attack of  $11^\circ$  and a Mach number of 0.85. As was shown in figure 2, a slight instability was obtained at a Mach number of 0.91. This instability occurred only at small values of  $pb/2V$ .

The  $60^\circ$  triangular wing shows a small region of hysteresis with a stable slope at the higher rolling velocities. These nonlinearities through zero and the hysteresis loops may not be too troublesome with regard to controllability where large rolling velocities are reached; however, they may cause undesirable dynamic stability characteristics. The hysteresis loop would also complicate the design of any automatic stabilizing equipment planned for such an airplane. It might also be expected that the instabilities shown may bear some relation to the wing-dropping problem under maneuvering conditions.

#### Effect of "Fixes"

Since a loss in damping in roll is known to be strongly associated with tip stalling - which also causes pitch-up for some wing plan forms - tests were made to determine whether devices which are known to alleviate pitch-up would also improve the damping in roll. One such device, a leading-edge notch of  $0.02b/2$  width and  $0.08c$  depth, located at  $0.60b/2$

was tried on the  $60^\circ$  triangular wing and the results are shown in figure 5. This device effectively eliminated both the pitch-up and the damping-in-roll instability within the test Mach number range ( $M = 0.7$  to  $0.91$ ).

The effect of fences on the  $45^\circ$  swept wing is shown in figure 6. The fences extended the length of the chord and were located at the  $0.65b/2$  station. As can be seen, at a Mach number of  $0.85$  the fences delayed the pitch-up by some  $5^\circ$  and materially improved the damping. However at a Mach number of  $0.91$  the effectiveness of the fences on either the damping or the pitch-up decreased considerably.

#### Span-Load Distributions in Roll

In an effort to better understand the forces and distribution of forces contributing to the damping in roll, pressure-distribution measurements during roll were obtained on the  $45^\circ$  sweptback wing. The results at a Mach number of  $0.85$  and at angles of attack of  $0^\circ$  and  $13^\circ$  are shown in figure 7. Comparisons of the measured and estimated values of the spanwise load coefficient due to roll are given in the upper part of the figure for  $\alpha = 0^\circ$ . A similar comparison but applied only to the increment due to roll for  $\alpha = 13^\circ$  is given in the lower part of the figure. In both cases the agreement between measured and estimated results is quite good. The estimation involved use of measured pressure distributions in pitch, which can be obtained by a relatively simple technique and for which considerable published data are available (refs. 26 and 27). The measurement of pressure distributions during rolling, on the other hand, requires the use of complex equipment. Numerous possibilities for errors or leakage exist and, at best, the precision of the resulting data is only fair.

The procedure for making the estimation is illustrated in figure 8. The local section normal-force curves are presented for spanwise stations of 40, 80, and 95 percent semispan. The increment of angle of attack due to roll at any spanwise station is given by

$$\Delta\alpha = 57.3 \frac{pb}{2V} \frac{y}{b/2} K$$

where  $K$ , the correction factor which takes into account the difference in aerodynamic induction for the angle-of-attack and rolling conditions, was derived from reference 28 and is given by the expression

$$K = \frac{2 + \sqrt{4 + \frac{A^2}{\cos^2 \Lambda}}}{4 + \sqrt{16 + \frac{A^2}{\cos^2 \Lambda}}}$$

The variation of the value of  $K$  with taper ratio, as well as the spanwise variation of  $K$ , has been investigated by using unpublished symmetrical and antisymmetrical loading data computed by the 15-point method of Weissinger (ref. 29). The effects of taper and the spanwise variation of  $K$  were found to be small and it therefore appears that the equation given here can be used for all plan forms.

The angle of attack for the wing at zero rolling velocity and for the upgoing and downgoing wing panels at a rolling velocity equivalent to  $\frac{p_b}{2V} = 0.06$  are indicated in figure 8. The increment of spanwise load coefficient due to rolling is merely the difference in section normal-force coefficient (multiplied by the appropriate chord ratio) between the angle of attack for  $\frac{p_b}{2V} = 0$  and  $\frac{p_b}{2V} = 0.06$ , as indicated in figure 8.

As is shown in figure 7 this procedure yields results that are in good agreement at both low and high angles of attack. Because of the difficulties of obtaining pressures in roll, it is felt that an estimation procedure of the type outlined may be the more practical approach in most instances.

#### CONCLUDING REMARKS

An investigation of the damping-in-roll characteristics of four wings at Mach numbers up to 0.91 and at angles of attack up to  $13^\circ$  indicates that a serious loss in damping generally occurs at successively lower angles of attack as the Mach number is increased. For swept wings which are subject to pitch-up tendencies, loss of damping in roll normally occurs at about the angle of attack for pitch-up and those devices which alleviate pitch-up are similarly effective in improving the damping in roll. Also, the increment of span load distribution due to roll can be satisfactorily estimated if measured pressure-distribution data in pitch are available.

Langley Aeronautical Laboratory,  
National Advisory Committee for Aeronautics,  
Langley Field, Va., June 25, 1953.

## REFERENCES

1. Goodman, Alex, and Adair, Glenn H.: Estimation of the Damping in Roll of Wings Through the Normal Flight Range of Lift Coefficient. NACA TN 1924, 1949.
2. Tosti, Louis P.: Low-Speed Static Stability and Damping-in-Roll Characteristics of Some Swept and Unswept Low-Aspect-Ratio Wings. NACA TN 1468, 1947.
3. Brewer, Jack D., and Fisher, Lewis R.: Effect of Taper Ratio on the Low-Speed Rolling Stability Derivatives of Swept and Unswept Wings. NACA TN 2555, 1951.
4. Goodman, Alex, and Fisher, Lewis R.: Investigation at Low Speeds of the Effect of Aspect Ratio and Sweep on Rolling Stability Derivatives of Untapered Wings. NACA Rep. 968, 1950 (Supersedes NACA TN 1835.)
5. Jaquet, Byron M., and Brewer, Jack D.: Effects of Various Outboard and Central Fins on Low-Speed Static-Stability and Rolling Characteristics of a Triangular-Wing Model. NACA RM L9E18, 1949.
6. Jaquet, Byron M., and Brewer, Jack D.: Low-Speed Static-Stability and Rolling Characteristics of Low-Aspect-Ratio Wings of Triangular and Modified Triangular Plan Forms. NACA RM L8L29, 1949.
7. Hunton, Lynn W., and Dew, Joseph K.: Measurements of Damping in Roll of Large-Scale Swept-Forward and Swept-Back Wings. NACA RM A7D11, 1947.
8. Sanders, E. Claude, Jr.: Damping in Roll of Straight and  $45^{\circ}$  Swept Wings of Various Taper Ratios Determined at High Subsonic, Transonic, and Supersonic Speeds With Rocket Powered Models. NACA RM L51H14, 1951.
9. Sanders, E. Claude, Jr., and Edmondson, James L.: Damping in Roll of Rocket Powered Test Vehicles Having Swept, Tapered Wings of Low Aspect Ratio. NACA RM L51G06, 1951.
10. Bland, William M., Jr., and Dietz, Albert E.: Some Effects of Fuselage Interference, Wing Interference, and Sweepback on the Damping in Roll of Untapered Wings as Determined by Techniques Employing Rocket-Propelled Vehicles. NACA RM L51D25, 1951.
11. Edmondson, James L.: Damping in Roll of Rectangular Wings of Several Aspect Ratios and NACA 65A-Series Airfoil Sections of Several Thickness Ratios at Transonic and Supersonic Speeds as Determined With Rocket-Powered Models. NACA RM L50E26, 1950.

12. Sanders, E. Claude, Jr.: Damping in Roll of Models with  $45^\circ$ ,  $60^\circ$ , and  $70^\circ$  Delta Wings Determined at High Subsonic, Transonic, and Supersonic Speeds With Rocket-Powered Models. NACA RM L52D22a, 1952.
13. Brown, Clinton E., and Heinke, Harry S., Jr.: Preliminary Wind-Tunnel Tests of Triangular and Rectangular Wings in Steady Roll at Mach Numbers of 1.62 and 1.92. NACA RM L8L30, 1949.
14. McDearmon, Russel W., and Heinke, Harry S., Jr.: Investigation of the Damping in Roll of Swept and Tapered Wings at Supersonic Speeds. NACA RM L53A13, 1953.
15. Martin, John C., and Gerber, Nathan: On the Effect of Thickness on the Damping in Roll of Airfoils at Supersonic Speeds. Rep. No. 843, Ballistic Res. Lab., Aberdeen Proving Ground, Jan. 1953.
16. Bolz, Ray E., and Nicolaides, John D.: A Method of Determining Some Aerodynamic Coefficients from Supersonic Free-Flight Tests of a Rolling Missile. Jour. of Aero. Sci. vol. 17, no. 10, Oct. 1950, pp. 609-621.
17. Nicolaides, John D., and Bolz, Ray E.: On the Pure Rolling Motion of Winged or Finned Missiles in Varying Supersonic Flight. Rep. No. 799, Ballistic Research Laboratory, Aberdeen Proving Ground, Mar. 1952.
18. Lockwood, Vernard E.: Effects of Sweep on the Damping-In-Roll Characteristics of Three Sweptback Wings Having an Aspect Ratio of 4 at Transonic Speeds. NACA RM L50J19, 1950.
19. Kuhn, Richard E., and Myers, Boyd C., II.: Effects of Mach Number and Sweep on the Damping-in-Roll Characteristics of Wings of Aspect Ratio 4. NACA RM L9E10, 1949.
20. Myers, Boyd C., II, and Kuhn, Richard E.: High-Subsonic Damping-in-Roll Characteristics of a Wing with the Quarter-Chord Line Swept Back  $35^\circ$  and With Aspect Ratio 3 and Taper Ratio 0.6. NACA RM L9C23, 1949.
21. Kuhn, Richard E., and Wiggins, James W.: Wind-Tunnel Investigation of the Aerodynamic Characteristics in Pitch of Wing-Fuselage Combinations at High Subsonic Speeds. Aspect Ratio Series. NACA RM L52A29, 1952.
22. Kuhn, Richard E., and Wiggins, James W.: Wind-Tunnel Investigation to Determine the Aerodynamic Characteristics in Steady Roll of a Model at High Subsonic Speeds. NACA RM L52K24, 1953.

- 23. Gillis, Clarence L., Polhamus, Edward C., and Gray, Joseph L., Jr.: Charts for Determining Jet-Boundary Corrections for Complete Models in 7- by 10-Foot Closed Rectangular Wind Tunnels. NACA WR L-123, 1945. (Formerly NACA ARR L5G31.)
- 24. Hensel, Rudolf W.: Rectangular-Wind-Tunnel Blocking Corrections Using the Velocity-Ratio Method. NACA TN 2372, 1951.
- 25. Wolhart, Walter D.: Influence of Wing and Fuselage on the Vertical-Tail Contribution to the Low-Speed Rolling Derivatives of Midwing Airplane Models With  $45^\circ$  Sweepback Surfaces. NACA TN 2587, 1951.
- 26. Loving, Donald L., and Williams, Claude V.: Aerodynamic Loading Characteristics of a Wing-Fuselage Combination Having a Wing of  $45^\circ$  Sweepback Measured in the Langley 8-Foot Transonic Tunnel. NACA RM L52B27, 1952.
- 27. Solomon, William, and Schmeer, James W.: Effect of Longitudinal Wing Position on the Pressure Characteristics at Transonic Speeds of a  $45^\circ$  Sweptback Wing-Fuselage Model. NACA RM L52K05a, 1953.
- 28. Diederich, Franklin W.: A Plan-Form Parameter for Correlating Certain Aerodynamic Characteristics of Swept Wings. NACA TN 2335, 1951.
- 29. Weissinger, J.: The Lift Distribution of Swept-Back Wings. NACA TM 1120, 1947.

TABLE I.- GEOMETRIC CHARACTERISTICS OF THE MODELS INVESTIGATED

Sweep angle, deg	Aspect ratio	Taper ratio	Airfoil section	Reynolds number based on $\bar{c}$
3.6 at $c/4$	4	0.6	65A006	$1.8 \times 10^6$ to $3.0 \times 10^6$
32.6 at $c/4$	4	0.6	65A006	$1.8 \times 10^6$ to $3.0 \times 10^6$
45 at $c/4$	4	0.6	65A006	$1.8 \times 10^6$ to $3.0 \times 10^6$
60 at L.E.	2.31	0	65A003	$3.1 \times 10^6$ to $5.2 \times 10^6$



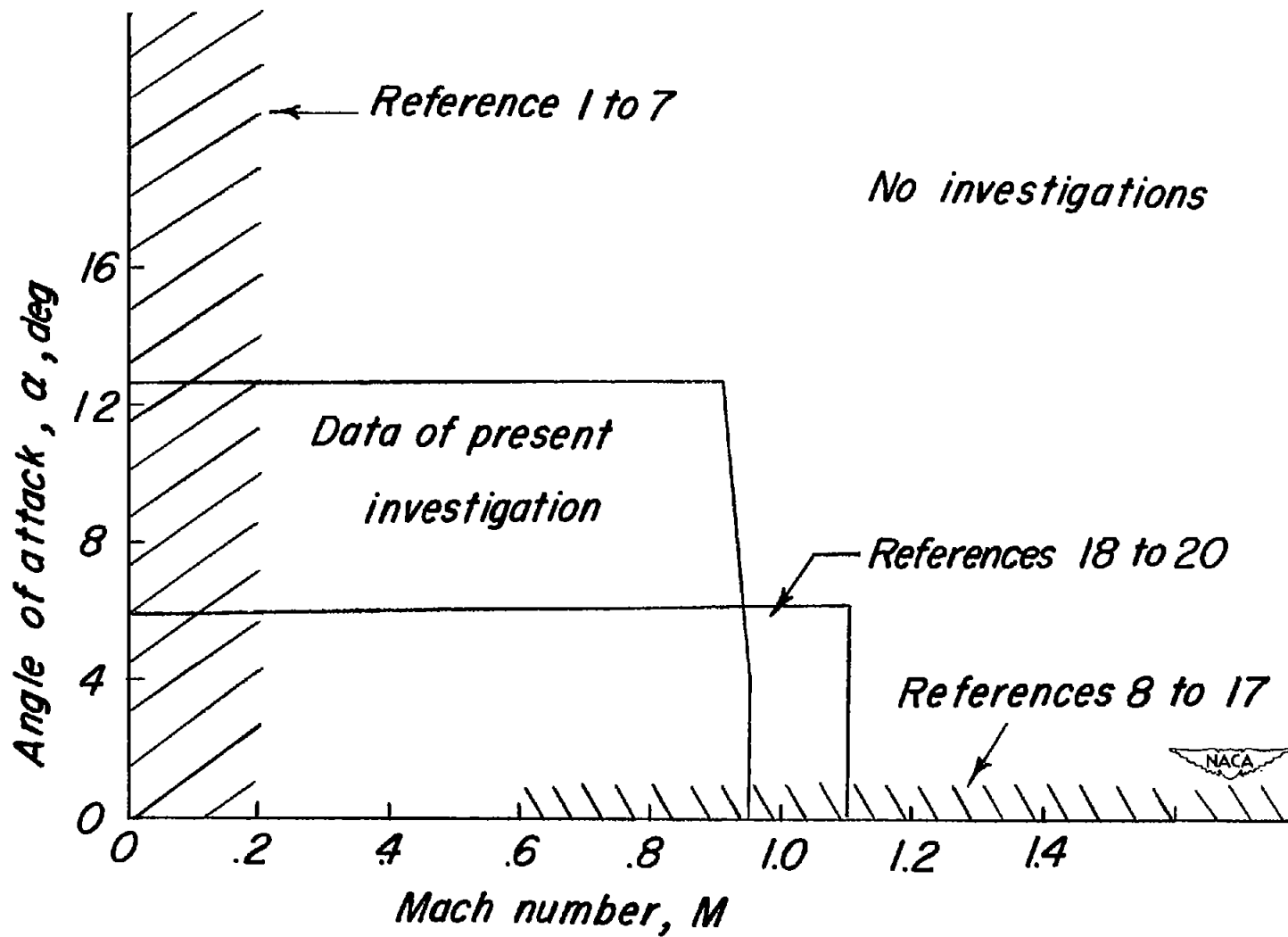


Figure 1.- Ranges of Mach number and angle of attack covered in damping-in-roll investigations.

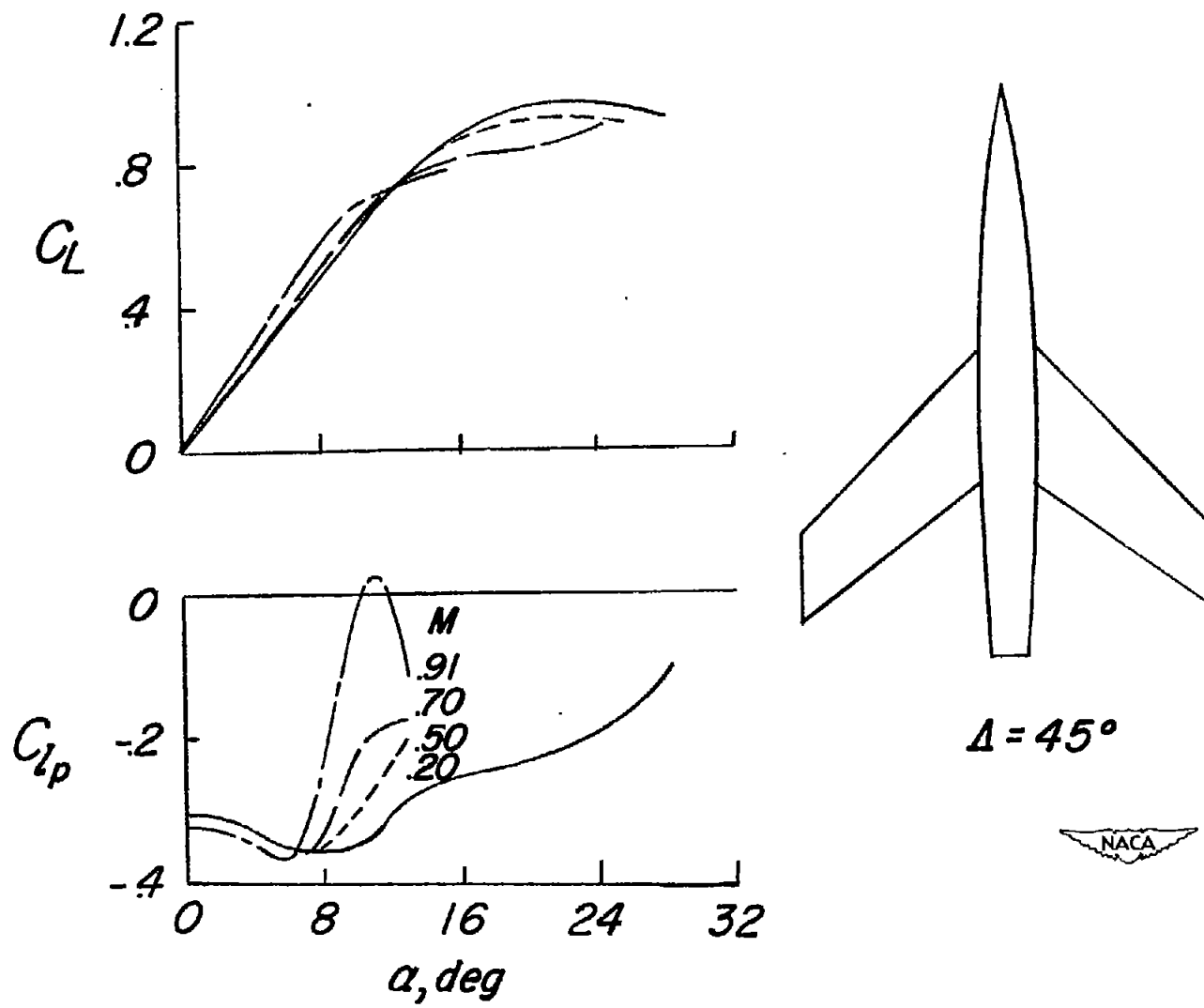


Figure 2.- Variation of the damping-in-roll derivative  $C_{l_p}$  with Mach number and angle of attack.

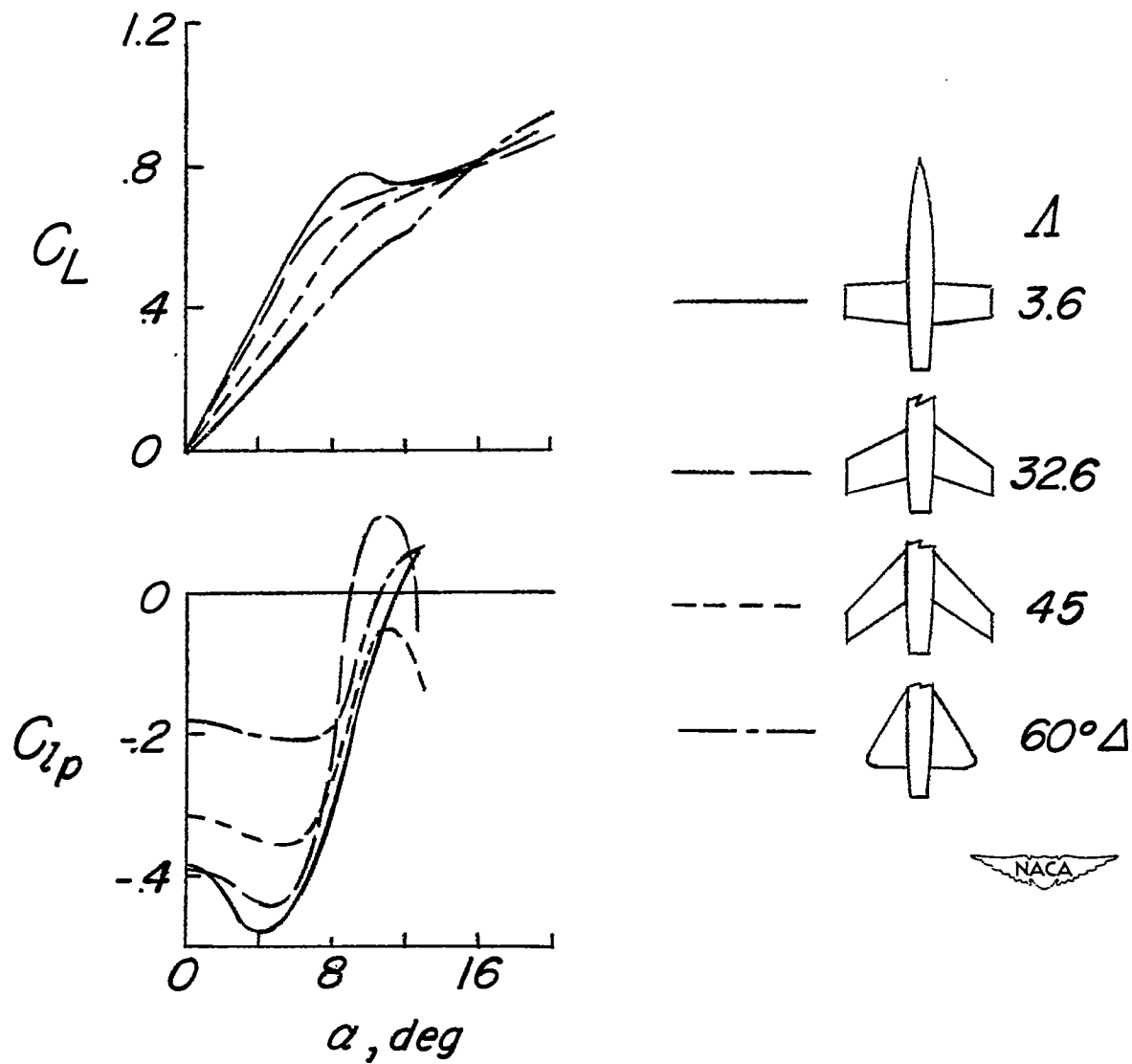


Figure 3.- Variation of the damping-in-roll derivative  $C_{l_p}$  with angle of attack.  $M = 0.85$ .

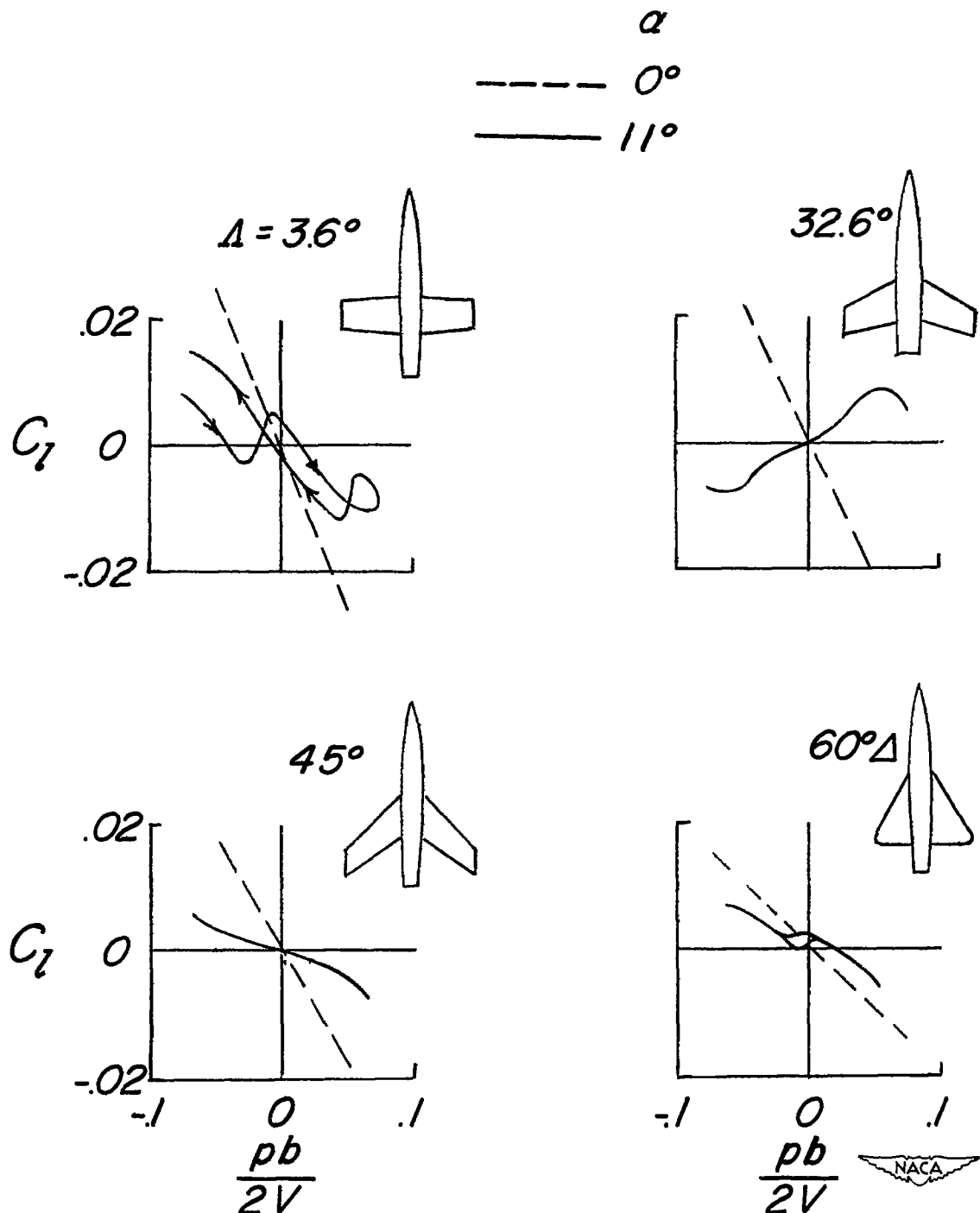


Figure 4.- Some typical variations of the rolling-moment coefficient  $C_l$  with the rate of roll  $pb/2V$ .  $M = 0.85$ .

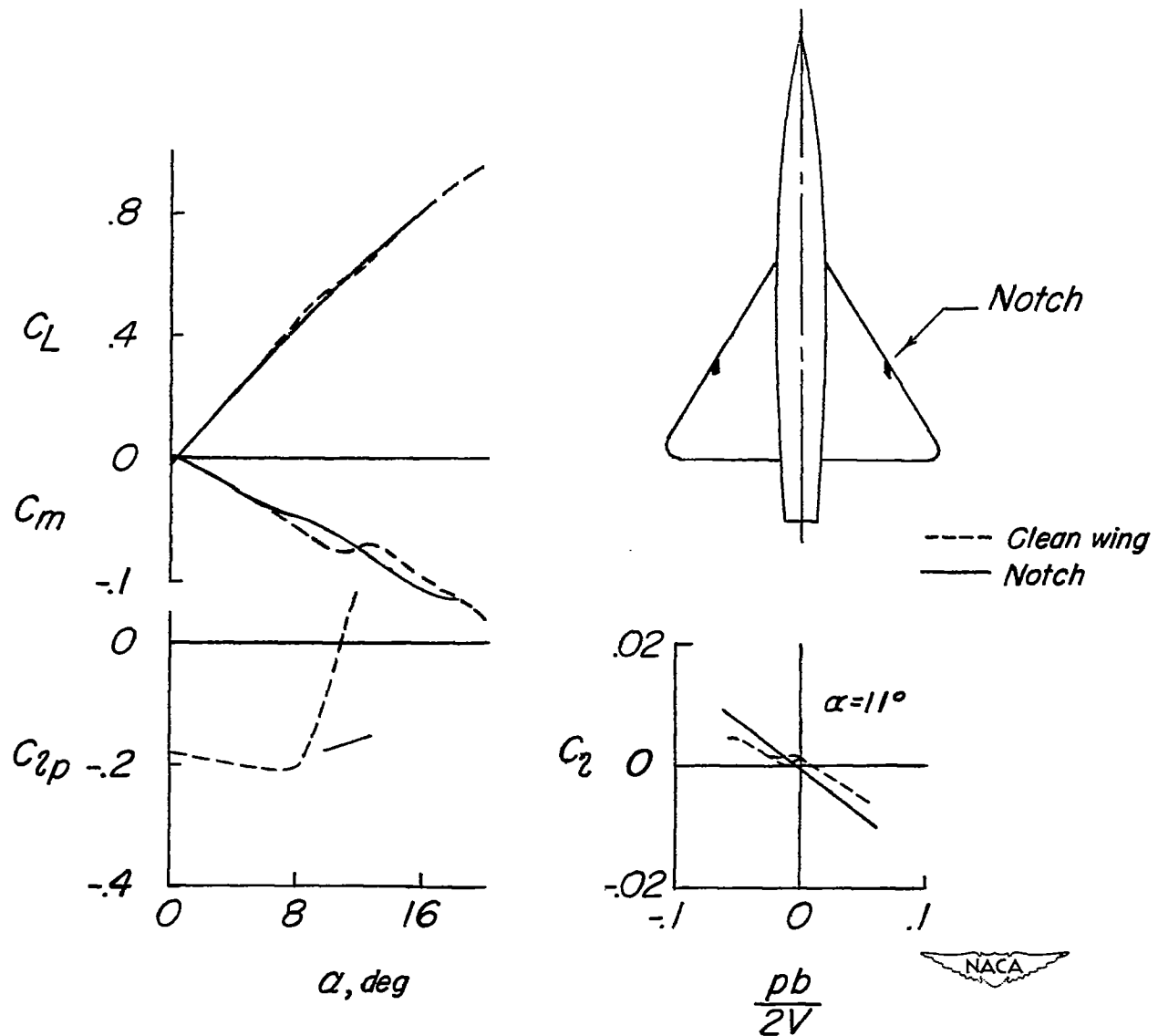


Figure 5.- Effect of notches on the characteristics of the  $60^\circ$  triangular wing.  $M = 0.85$ .

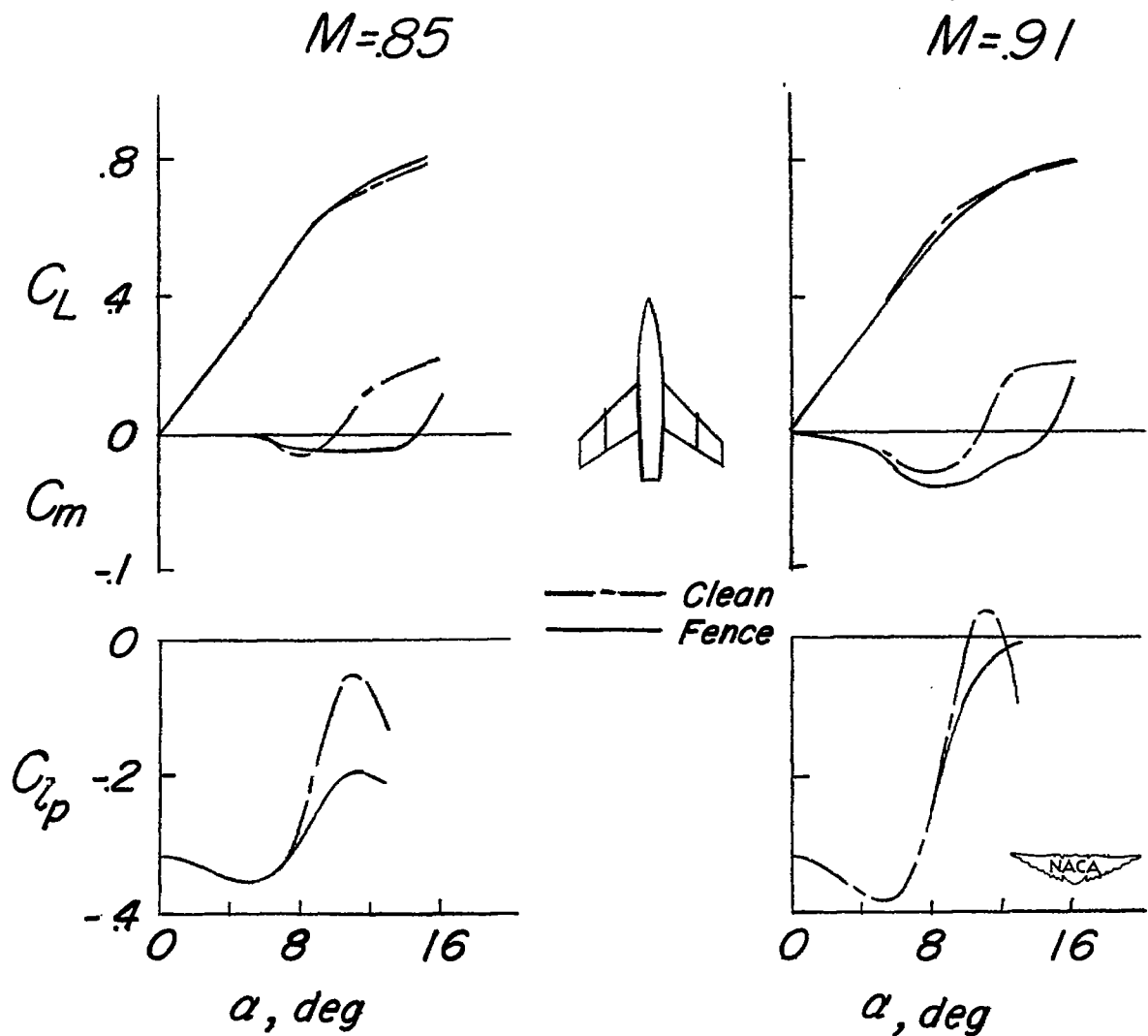


Figure 6.- Effect of fences on the characteristics of the  $45^\circ$  swept wing.

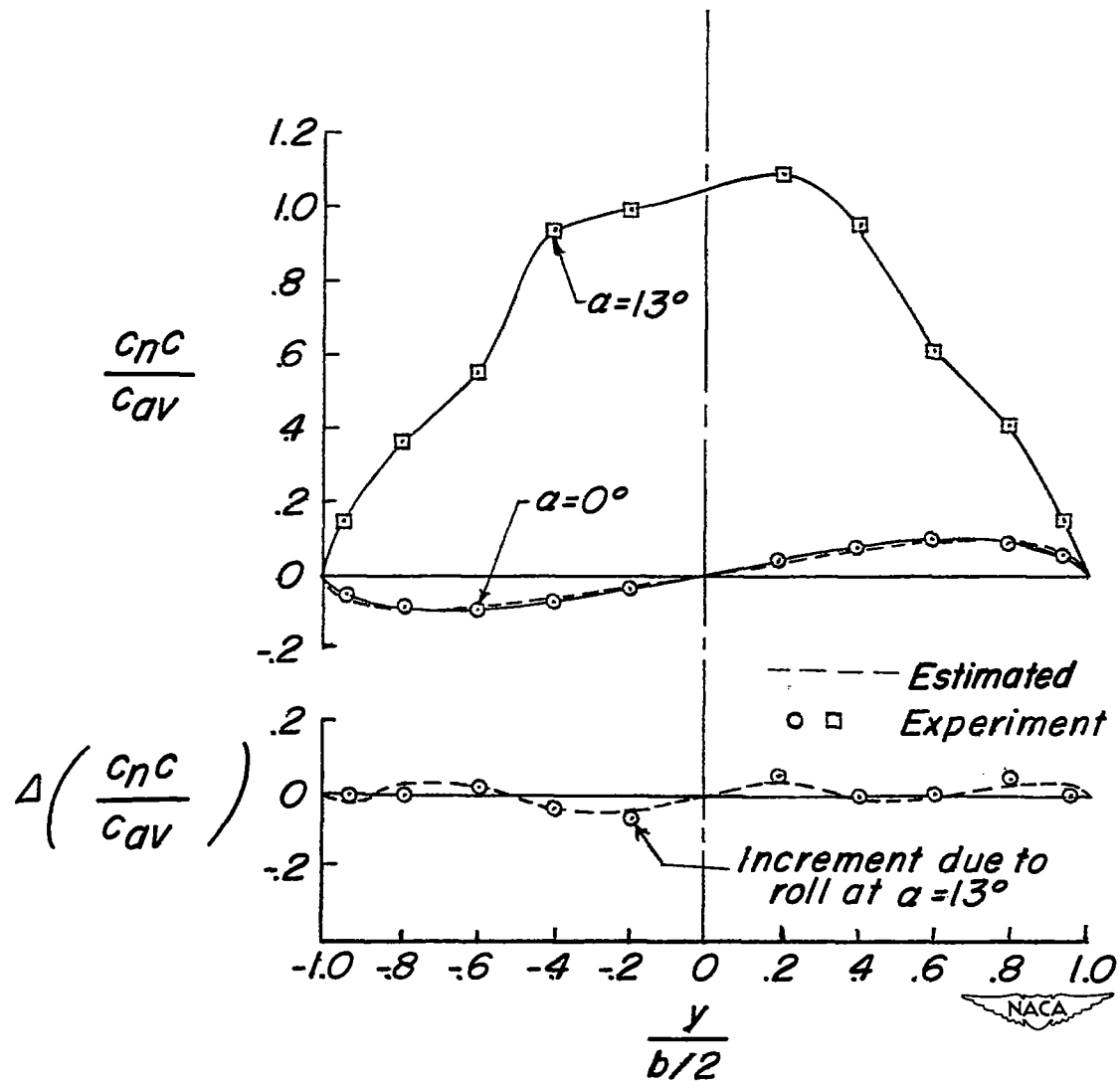


Figure 7.- Comparison of measured and estimated distribution of load on the  $45^\circ$  swept wing while rolling.  $M = 0.85$ ;  $\frac{pb}{2V} = 0.06$ .

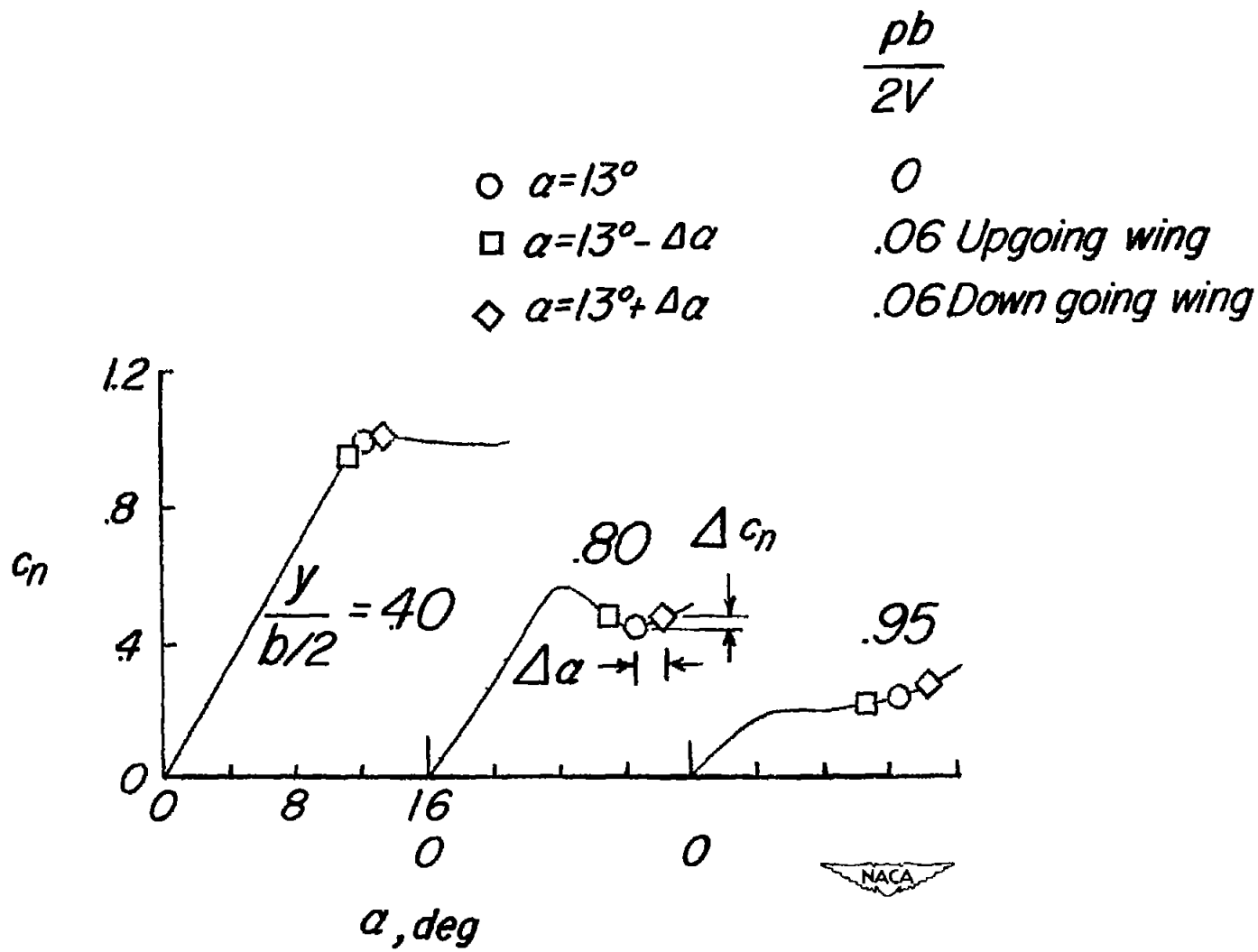


Figure 8.- Illustration of the method used to estimate the increment of span-load distribution due to roll.  $M = 0.85$ .